# Statistical properties of poloidal transport in zonal flows with finite Larmor radius effects

Hector A. Velasco and Julio J. Martinell

*Instituto de Ciencias Nucleares, UNAM, A. Postal 70-543, México D.F., Mexico*

**I. Introduction.** A simple description of drift wave transport in presence of a zonal flow uses the dynamics of a test particle described by a Hamiltonian system which is liable to present chaotic behavior when the fluctuation amplitude is large. The zonal flow is manifested by the presence of a barrier to radial transport. To zeroth order in the particle Larmor radius the effect of the transport barrier in isolating the central plasma is erased for large enough fluctuation level. However, the inclusion of finite Larmor radius effects has been found to restore the barrier [1]. This is important for alpha particle confinement since it indicates that they are affected by a transport barrier even for large fluctuation levels. Another interesting problem is whether the type of transport is diffusive or not. This can sometimes be inferred from the statistical properties of transport since the variance of the particle distribution may exhibit a nonlinear dependence with time. In this work we have analyzed the statistical behavior of a large group of test particles in order to determine the resulting probability distribution function (PDF) for displacements in the poloidal direction, i.e. parallel to the transport barrier in non-monotonic zonal flows (non-twist Hamiltonian) taking into account finite Larmor radius (FLR) effects.

**II. Test particle model with FLR effects.**

Consider a test particle subject to the $E \times B$ drift velocity, with $B$ along the $z$ direction, which assumes that the particle follows the guiding center velocity. For finite gyroradii the particle actually samples spatial regions around the guiding center and this effect can be accounted for by taking the average of the drift equations over the gyroradius. Thus, the equations are

$$\frac{dx}{dt} = -\left\langle \frac{\partial \phi}{\partial y} \right\rangle_\theta , \qquad \frac{dy}{dt} = \left\langle \frac{\partial \phi}{\partial x} \right\rangle_\theta \tag{1}$$

where the gyroaverage, $\langle\rangle_\theta$, is defined as $\langle \Psi \rangle_\theta \equiv \frac{1}{2\pi}\int_0^{2\pi} \Psi(x+\rho\cos\theta, y+\rho\sin\theta)\, d\theta$ . $x$ and $y$ are radial and poloidal coordinates. This represents a Hamiltonian system with $\langle\phi\rangle_\theta$ as the Hamiltonian. In our model $\phi = \phi_0 + \phi_1$ where $\phi_0$ is the zonal flow, given by $\hat{u}_0(x) = \frac{d\phi_0}{dx} = \mathrm{sech}^2 x$, and the fluctuations $\phi_1$ are given by two modes of the Hasegawa-Mima equation, in the co-moving frame of one mode. Its gyroaverage is,

$$\langle\phi\rangle_\theta = J_{0\rho}(x) - \eta x + \varepsilon_1 J'_{k_1\rho}(x)\cos(k_1 y) + \varepsilon_2 J'_{k_2\rho}(x)\cos(k_2 y - \omega t)\,, \tag{2}$$

where the prime denotes the derivative of the function $J_{k\rho}(x)$, which is defined by,

$$J_{k,\rho}(x) = \frac{1}{\pi}\int_0^{\pi} \tanh\left(x+\rho\cos\theta\right)\cos\left(k\rho\sin\theta\right)d\theta\,. \tag{3}$$

The equations 1 with 2 are integrated to determine the particle evolution. When $\varepsilon_2 = 0$ the system is time independent and the phase space (in our case the $x-y$ space) has integral surfaces. In general, it is characterized by two resonances on each side of the shearless point, where the mode velocity equals the flow velocity. For $\rho = 0$ the resonances can form two sepparate chains of islands (heteroclinic, when wave amplitude is low, see Fig. 1) or they can join in coupled chains (homoclinic, for large wave amplitude). For finite $\rho$ the island chains separation grows with $\rho$ and eventualy a bifurcation occurs that forms 4 island chains. When $\varepsilon_2 \neq 0$ the system is non integrable and chaotic regions appear near rational surfaces, which widen as $\varepsilon_2$ grows. But the shearless curve (between the islands) acts as a barrier that particles cannot cross until $\varepsilon_2$ exceeds a certain threshold that depends nonlinearly on $\rho$ [1]. Chaoric transport is thus limited by this transport barrier in radial ($x$) direction. On the other hand, poloidal ($y$) transport is not blocked by this effect and is thus interesting to study its properties in the non-twist Hamiltonian associated with the radial barrier. The statistical properties in the twist case (no barrier) were studied in [2] and in [3] including FLR effects.

**III. Transport properties.**

In order to study the nature of transport in $y$ direction we place a large number of particles centered around the hyperbolic point of Fig. 1 and let them evolve for a sufficiently long time. They comprise closed and open orbits in comparable proportions. Typically we use about $10^4$ particles but sometimes larger numbers are required to separate the different populations. The integrations are lengthy but we can take advantage of the independence of particle trajectories to perform parallel computations. Therefore we use GPU parallel programming based on CUDA in order to speed up the process. With this technique, execution times are found to improve by a factor of up to 100. In this way, the PDFs can be efficiently found. The behavior depends on the values of the parmeters $\varepsilon_1, \varepsilon_2$ and $\rho$. There are three types of particle trajectories: (1) trapped in the islands (2) free-streaming that flow unhindered along $y$ and (3) trapped-flight which alternate between the two (the most common, also called sticky-flight). For

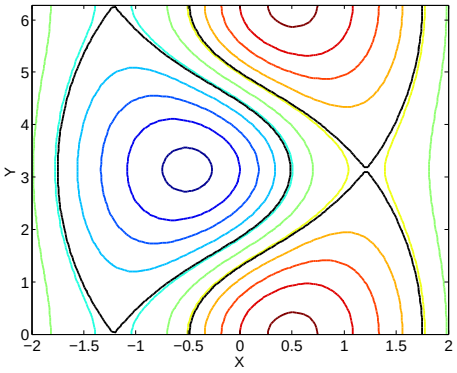


Figure 1: Topology of phase space.

non chaotic cases ($\varepsilon_2 = 0$) only the first two populations are present and are clearly separated; the orbits are deterministic. The distribution functions along $y$ are shown in Fig. 2. For $\varepsilon_2 \neq 0$ chaotic transport produce sticky-flight orbits and the distribution fuctions are wider as seen in Fig. 3.

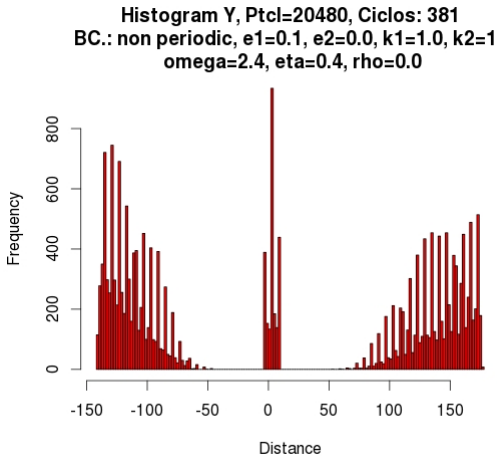


Figure 2: Distribution function of particles with non chaotic orbits.

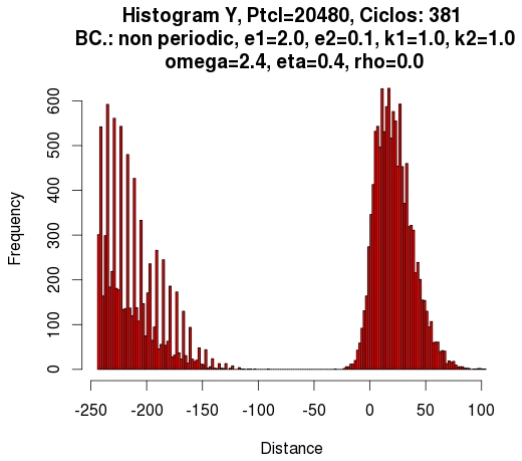


Figure 3: Patricle distribution function with chaotic orbits.

The population that stays near zero usually keeps the local coherence, while those that travel to the left or right display quite different behaviors. The figures presented give a sample of this variety. Usually one of the two extremes can have a more coherent shape and that is the one most commonly analyzed here. When the dispersion in particles looks wild the analysis cannot be performed.

The interesting property to follow is the width of the distribution as this is a meassure of the statistical spread that determines the transport type. Thus the variance $\sigma$ of the distribution of a single population is analyzed and its time dependence is determined. For diffusive transport the linear relation $\sigma \propto t$ is satisfied. However, nondiffusive behaviors have a nonlinear dependence of the type $\sigma \propto t^{\gamma}$. When this is done in the cases with chaos it is generally found that $\gamma \approx 2$ which is indicative of superdiffusive transport.

Another important charcteristic of the transport is the form of the probability distribution function (PDF). For diffusive transport the PDF is Gaussian. However, for some cases here when $\varepsilon_2 \neq 0$ they are not Gaussian, but present tails that decay more slowly. This is evidence for non-diffusive transport. This can be seen in Figs. 4 and 5 where the two types of distributions are obtained. The first case, with large $\varepsilon_2$ chaos level is high and the PDF is Gaussian since the information about trapped or free orbits is lost. In the second case the PDF is non Gaussian hav-

ing a long tail on the right side. The tail is realted to the presence of long flights in some orbits. Trapping and circulating events in the particles trajectories are equivalent to Levy flights. It has been found that the long tails are described by Levy distributon functions [4] which asymptotically have the dependence $F \propto x^{-\mu}$. For a Levy-type PDF it is required that the exponent $\mu < 3$, so that the decay is slow enough. In the cases analyzed we have several situations with $\mu < 3$ although it is difficult to assign a value due to the complicated PDFs found.

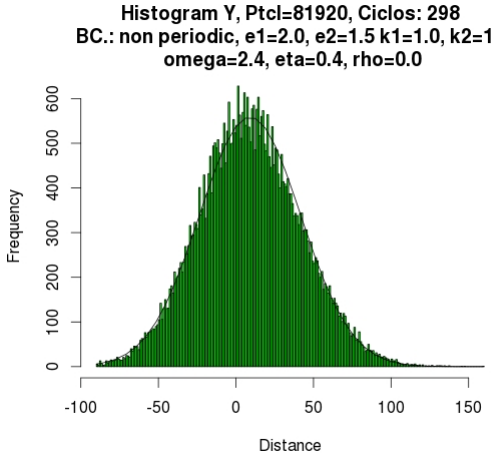


Figure 4: PDF with high level of chaos with a Gaussian-like behavior.

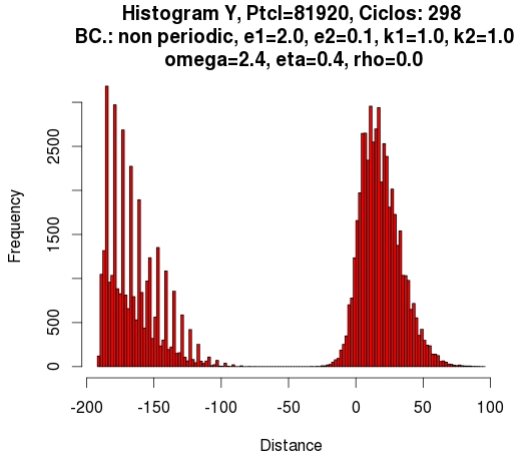


Figure 5: PDF with non-Gaussian distribution in the far population.

The effect of FLR is to increase the non-local effects, i.e. large values of $\rho$ usually have lower values of $\mu$. The results of having a bifurcation in the phase-space topology (for $\rho > 2.33$) is to increase the degree of left right anisotropy. From the analysis we can conclude that the nondiffusive transport found for the cases of Hamiltonian systems with twist is preserved for non-twist systems. In particular the superdiffusive nature and the non-Gaussian PDF. FLR effects are not very noticeable although they modify quantitatively the transport.

**Acknowledgements.** This work was partially supported by projects DGAPA-UNAM IN106911, IN109115 and CONACyT 152905.

## References

[1] J.J. Martinell and D. del-Castillo-Negrete, Phys. Plasmas **20**, 022303 (2013)

[2] D. del-Castillo-Negrete, Phys. Plasmas **7**, 1702 (2000).

[3] K. Gustafson, D. del-Castillo-Negrete and W. Dorland, Phys. Plasmas **15**, 102309 (2008).

[4] D. del-Castillo-Negrete, Phys. Fluids **10**, 576 (1998).